Biomaterials 276 (2021) 121031

Contents lists available at ScienceDirect

Biomaterials

journal homepage: www.elsevier.com/locate/biomaterials

Core-shell hydrogel microfiber-expanded pluripotent stem cell-derived lung progenitors applicable to lung reconstruction *in vivo*

Satoshi Ikeo [a], Yuki Yamamoto [b,c], Kazuhiro Ikeda [d], Naoyuki Sone [a], Yohei Korogi [a], Lucia Tomiyama [b], Hisako Matsumoto [a], Toyohiro Hirai [a], Masatoshi Hagiwara [e], Shimpei Gotoh [a,b,*]

[a] Department of Respiratory Medicine, Graduate School of Medicine, Kyoto University, Kyoto, 606-8507, Japan
[b] Department of Drug Discovery for Lung Diseases, Graduate School of Medicine, Kyoto University, Kyoto, 606-8501, Japan
[c] HiLung Inc., Kyoto, 606-8304, Japan
[d] CellFiber Co., Ltd, Tokyo, 113-8485, Japan
[e] Department of Anatomy and Developmental Biology, Graduate School of Medicine, Kyoto University, Kyoto, 606-8501, Japan

ARTICLE INFO

Keywords:
Pluripotent stem cells
Lung progenitors
Core-shell hydrogel microfibers
Three-dimensional cell culture
Xenotransplantation
Regenerative medicine

ABSTRACT

Lung transplantation is the only treatment available for end-stage lung diseases; however, donor shortage is a global issue. The use of human pluripotent stem cells (hPSCs) for organ regeneration is a promising approach. Nevertheless, methods for the expansion of isolated hPSC-derived lung progenitors (hLPs) for transplantation purposes have not yet been reported. Herein, we established an expansion system of hLPs based on their three-dimensional culture in core-shell hydrogel microfibers, that ensures the maintenance of their bipotency for differentiation into alveolar and airway epithelial cells including alveolar type II (AT2) cells. Further, we developed an efficient *in vivo* transplantation method using an endoscope-assisted transtracheal administration system; the successful engraftment and *in vivo* differentiation of hLPs into alveolar epithelial cells (incorporated into the alveoli) was observed. Importantly, expanded hLPs in the context of microfibers were successfully transplanted into the murine lungs, opening avenues for cell-based therapies of lung diseases. Therefore, our novel method has potential regenerative medicine applications; additionally, the high-quality hLPs and AT2 cells generated via the microfiber-based technology are valuable for drug discovery purposes.

1. Introduction

Lung transplantation is the ultimate treatment option for end-stage lung diseases [1], such as chronic obstructive pulmonary disease, pulmonary fibrosis, and other refractory lung diseases. However, the lack of donors and the strict indication criteria results in the eventual death of many patients [2]; therefore, there is a high demand and necessity for alternative therapeutic approaches, including cell-based therapies [3]. While mesenchymal stromal cells, endothelial progenitors, and adipose-derived stem cells have all been employed in cell-based therapies, such treatments were used for immunomodulatory and paracrine effects [4], and not for lung reconstruction. In addition, various clinical trials have reported the safety of cell-based therapies [5,6], but not their effectiveness [7]. Of note, although lung epithelial stem cells are essential for lung regeneration [8], their obtention is challenging due to the difficulty of their expansion [9], and their potential for regenerative medicine purposes remains to be evaluated.

Recently, different methods for the induction of human pluripotent stem cell (hPSC)-derived lung progenitors (hLPs) and respiratory epithelial cells have been reported [10–15]. Besides, there have been reports of the transplantation of hPSC-derived cells into various human organs for therapeutic purposes [16,17]. However, considering cell-based therapies as medical procedures, scalable culture methods to obtain a sufficient number of cells were not reported thus far in the context of two-dimensional culture [18,19]. Of note, organoids containing lung progenitors were reported to be passageable maintaining their differentiation capacity [15,20–22]; however, the expansion of hLPs alone sorted using lung progenitor-specific markers has never been reported. Moreover, the robust transplantation of hLPs into the alveoli, whose injury is tightly associated with the pathogenesis of various intractable lung diseases, has never been described.

In this paper, we expanded hLPs in the context of scalable culture

* Corresponding author. 54 Kawaharacho, Shogoin, Sakyo-ku, Kyoto, 606-8507, Japan.
E-mail address: a0009650@kuhp.kyoto-u.ac.jp (S. Gotoh).

https://doi.org/10.1016/j.biomaterials.2021.121031
Received 8 February 2021; Received in revised form 2 June 2021; Accepted 14 July 2021
Available online 19 July 2021

without animal-derived scaffolds using cell-laden core-shell microfibers, reportedly applicable to regenerative medicine due to the highly efficient cell expansion potential and the easy retrieval of cultured cells maintaining the cell properties [23,24]. Here, the expanded hLPs via the microfiber system exhibited self-renewal ability and directly differentiated into both alveolar and airway lineage cells. Importantly, after the intratracheal administration of hLPs into the lungs of mice, their successful engraftment was observed; of note, hLPs differentiated *in vivo* into various respiratory cell lineages, including the alveolar type II (AT2) cell lineage. Furthermore, transplanted cells were incorporated into the murine lung parenchyma. Finally, we succeeded the transplantation of hLPs expanded using microfiber system. Overall, our results clearly suggest that hLPs expanded in microfibers can be useful for lung regeneration.

2. Materials and methods

2.1. Maintenance of human PSCs

The SFTPC-GFP reporter human induced pluripotent stem cell (hiPSC) line (B2-3) [10] derived from the 201B7 [25] hiPSC line, the mCherry expressing B2-3 (mB2-3) reporter hiPSC line, the 648A1 [26] hiPSC line, and the H9 [27] human embryonic stem cell (hESC) line were used in the current study. Each cell line was maintained without feeder cells in Essential 8 medium (Thermo Fisher Scientific, A1517001) under 5% CO_2 at 37 °C, as previously described [12]. Each cell line was routinely tested for mycoplasma contamination using the MycoAlert mycoplasma detection kit (Lonza, LT07-118) and no contamination was detected. The use of H9 hESCs was approved by the Ministry of Education, Culture, Sports, Science and Technology (MEXT), Japan.

2.2. Generation of mCherry-expressing hiPSCs

The pCAGGS-mCherry vector was generated via the replacement of the *EGFP* gene sequence of the pCAGGS-EGFP vector with the *mCherry* gene sequence obtained from the pmCherry-C1 Vector (Clontech, 632,524) using the In-Fusion HD Cloning Kit (Clontech, 639,648). The pCAGGS-mCherry vector was electroporated into 1.0×10^6 B^2-3 *SFTPC-GFP* knock-in reporter hiPSCs [10] using a NEPA 21 electroporator (poring pulse: pulse voltage, 125 V; pulse width, 5 ms; pulse number, 2; NEPA GENE). After several weeks, mCherry$^+$ cells were selected via flow cytometry and single-cell cloning was conducted.

2.3. Differentiation of human PSCs into hLPs

Each human PSC line was stepwise differentiated into NKX2-1$^+$ lung progenitors, as previously described [12,28]. A total of 1.2×10^6 feeder-free PSCs per well were seeded onto Geltrex-coated (Thermo Fisher Scientific, A1413202) 6-well plates with RPMI medium (Nacalai Tesque, 30,264–56) containing 100 ng/mL Activin A (Oriental Yeast, 47,154,000), 1 μM CHIR99021 (Axon Medchem, Axon 1386), 2% B27 supplement (Thermo Fisher Scientific, 17,504–001), and 50 U/mL penicillin-streptomycin (Thermo Fisher Scientific, 15,140–163). Y-27632 (LC laboratories, Y5301) was supplemented at 10 μM on day 0. The medium was replaced every two days. Sodium butyrate (Wako, 193–015,122) was supplemented at a concentration of 0.25 mM on day 1 and of 0.125 mM on days 2 and 4. From day 6 to day 10, the cells were treated with 100 ng/mL Noggin (Proteintech, HZ-1118) and 10 μM SB431542 (Wako, 198–16543) in Glutamax-supplemented DMEM/F12 basal medium (Thermo Fisher Scientific, 35,050–061) containing 2% B27 supplement, 50 U/mL of penicillin-streptomycin, 0.05 mg/mL L-ascorbic acid (Wako, 012–04802), and 0.4 mM monothioglycerol (Wako, 195–15791). From day 10 to day 14, the cells were treated with 20 ng/mL BMP4 (Proteintech, HZ-1045), all-trans retinoic acid (ATRA) (Sigma-Aldrich, R2625), and CHIR99021 in the basal medium. The optimized combinations of ATRA/CHIR99021 were 0.5 μM/3.5 μM (H9), 0.05 μM/3.0 μM (B2-3 and mB2-3), and 1.0 μM/2.5 μM (648A1). Finally, the cells were treated with 3 μM CHIR99021, 10 ng/mL FGF10 (PeproTech, 100–26), 10 ng/mL KGF (PeproTech, 100–19), and 20 μM DAPT (Wako, 049–33583) from day 14 to day 21. The cells were detached on day 21 and NKX2-1$^+$ lung progenitors were isolated, as previously described [12,28]. Mouse anti-human carboxypeptidase M (CPM) (Wako, 014–27501) and anti-mouse IgG microbeads (Miltenyi Biotec, 130-048-401) were used. Thereafter, NKX2-1$^+$ hLPs were isolated via magnetic sorting, as previously described [11].

2.4. Fibroblast-free hLP differentiation into AT2 cells

hLPs were differentiated into AT2 cells without feeder fibroblasts, as previously described [12]. The medium consisted of Ham's F12 (Wako, 087–08355) supplemented with 50 nM dexamethasone (Sigma-Aldrich, D4902), 100 μM 8-Br-cAMP (Biolog, B007-500), 100 μM 3-isobutyl-1--methylxanthine (Wako, 095–03413), 10 ng/mL KGF, 1% B-27 supplement, 0.25% BSA (Thermo Fisher Scientific, 15,260,037), 15 mM HEPES (Sigma-Aldrich, H0887), 0.8 mM calcium chloride (Wako, 036–19731), 0.1% ITS premix (Corning, 354,350), 50 U/mL penicillin-streptomycin, 3 μM CHIR99021, 10 μM SB431542, and 10 μM Y27632. A total of 2.0×10^5 isolated hLPs were suspended in 200 μL of the medium and seeded onto nonadherent surface plates. After two days, the cell aggregates were collected and centrifuged. The pellets were gently resuspended in 20 μL of growth factor reduced Matrigel (Corning, 354,230) and then incubated in 12-well cell culture plates with 1 mL of medium until day 7. Fibroblast-free alveolar organoids were dissociated with 0.1% trypsin/EDTA [0.25% trypsin/EDTA (Thermo Fisher Scientific, 25,200–072) diluted in 0.5 mM EDTA (DOJINDO, 345–01865)/PBS (Nacalai tesque, 14,249–24)], and the cells were retrieved.

2.5. Two-dimensional culture of hLPs

A proliferation medium containing 3 μM CHIR99021, 100 ng/mL FGF10, 10 ng/mL KGF, 20 μM DAPT, and 10 μM Y-27632 was prepared. A total of 2.0×10^5 isolated hLPs were suspended in 1 mL of the proliferation medium and plated onto 12-well cell culture plates. hLPs were passaged once after two weeks and retrieved with Accutase (Innovative Cell Technologies, AT104-500) after another two weeks. The medium was replaced every two days.

2.6. Fabrication of cell-encapsulated microfibers and hLP culture

A double coaxial microfluidic device was assembled with pulled glass capillaries, rectangular glass tubes, and custom-made three-way connectors. Using the microfluidic device, microfibers containing lung progenitors were fabricated as previously described [23,24]. In brief, a pre-gel solution of 1.0% I-1G Na-alginate (KIMICA, I-1G) in saline for the shell stream and a mixture of 100 mM calcium chloride (Nacalai Tesque, 06729–55) and 3% sucrose (Nacalai Tesque, 30,403–55) solution for the sheath stream were prepared. Isolated lung progenitors were diluted to a concentration of 2.0×10^5 cells per 20 μL (1.0×10^7 cells/mL) in the proliferation medium. The flow rates of the core, shell, and sheath stream were 50 μL/min, 200 μL/min, and 3.6 mL/min, respectively. Cell-encapsulated microfibers were cultured in the proliferation medium. After 4 weeks of culture, the expansion phase was finished, and the medium was changed after one washing step with saline; alveolar or airway differentiation medium was used. The alveolar differentiation medium was the same as the fibroblast-free differentiation medium. The airway differentiation medium consisted of PneumaCult-ALI Basal Medium (STEMCELL Technologies, ST-05001) supplemented with PneumaCult-ALI Supplement, PneumaCult-ALI Maintenance Supplement, 4 μg/mL heparin, 1 μM hydrocortisone, 10 μM DAPT, and 10 μM Y-27632 [11]. In the differentiation phase, microfibers were incubated for 14 days (alveolar differentiation) or 28 days (airway differentiation). The medium was replaced every two days in both the expansion and

differentiation phases.

2.7. Retrieval of cells from the microfibers and preparation of single-cell suspensions

Microfibers were washed with D-PBS (−) (Nacalai tesque, 14,249–24) and incubated in 0.5 mM EDTA/PBS at room temperature for 10 min, followed by treatment with Accumax (Innovative Cell Technologies, AM105-100) at 37 °C for 10 min.

2.8. Flow cytometry

Single-cell suspensions were stained with primary antibodies at 4 °C for 20 min. After two washing steps, the cells were stained with the respective secondary antibodies at 4 °C for 20 min. After another two washes, the cells were stained with live-dead cell stains: 1 μM propidium iodide (Nacalai tesque, 29,037–76) or 1 μM SYTOX Blue Dead Cell Stain (Thermo Fisher Scientific, S34857). Fluorescence-activated cell sorting (FACS) analysis was performed using a FACSAria III (BD Biosciences). The antibodies used are listed in Table S1. The percentage of SFTPC-GFP positive cells was measured in the context of 3–4 biological replicates from 3 to 4 independent experiments.

2.9. Animals

Adult male NOD/Shi-scid, IL-2Rγ KO Jic (NOG) mice (Central Institute for Experimental Animals) (7–10 weeks of age) were used in this study. All animal experiments were approved by the Animal Research Committee of Kyoto University.

2.10. Transplantation of hLPs into the murine lungs

Naphthalene (Sigma-Aldrich, 147,141-25G) was dissolved in corn oil at 20 mg/mL and injected intraperitoneally at 200 mg/kg weight 48 h before the transplantation of lung progenitors into the murine lungs. Naphthalene-injured mice were further subjected to 2.5 Gy total body irradiation in a Cesium-137 irradiator (Gammacell 40 Exactor) 4–6 h before transplantation.

B2-3 and mB2-3 iPSC lines were used for transplantation purposes. Lung progenitors isolated on day 21 were suspended in an alveolar differentiation medium, seeded onto poly-HEMA (Sigma-Aldrich, 192,066)-coated Elplasia plates (Corning, 4446), and, after two days, cell aggregates were collected. The diameter and depth of the microwells were 200 μm and 100 μm, respectively. Prior to the transplantation of microfiber-hLPs, the microfibers were washed with D-PBS (−), incubated in 0.5 mM EDTA/PBS at room temperature for 10 min, and chopped into small pieces via gently pipetting. Cell aggregates were resuspended in a mixture of 50 μL of alveolar differentiation medium and 50 μL of Matrigel; the total volume of the aggregates' suspension was 100 μL. NOG mice were then anesthetized using a mixture of 0.3 mg/kg weight medetomidine (Wako, 139–17471), 4 mg/kg weight midazolam (Teva Takeda Pharma Ltd., 4987-123-40954-4), and 5 mg/kg weight butorphanol (Wako, 021–19001). The endoscope system for animals "TESALA AE-C1" (AVS) was used for the administration of cell aggregates into the murine lungs. The outer cylinder of the indwelling needle was placed into the left main bronchus under the endoscope and the cell suspension was administered from the outer cylinder. After cell transplantation, mice were awakened using 0.3 mg/kg weight atipamezole (Wako, 015–25331). Of note, the vehicle group received 50 μL of alveolar differentiation medium and 50 μL of Matrigel without any cells via the same procedure.

2.11. Transplantation of hLPs into the murine kidney capsule

As described above, cell aggregates were fabricated from a total of 1.0×10^7 lung progenitors and resuspended in 30 μL Matrigel. NOG male mice were anesthetized as described above, and a cell aggregates' suspension was transplanted into their left kidney capsule.

2.12. Analysis of the lungs of humanized mice

Lung dissociation. Three transplanted mice were used per independent experiment for this analysis; the experiment was repeated to obtain biological triplicates. Murine lung tissues were incubated with 2 U/mL Dispase II (Wako, 383–02281), 1 mg/mL collagenase/Dispase (Sigma-Aldrich, 10,269,638,001), and 0.1 mg/mL DNase I (Sigma-Aldrich, D4527) for 30 min at 37 °C and dissociated using the gentleMACS Dissociator (Miltenyi Biotec). After filtering through a 100 μm mesh, the cell suspension was treated with ACK lysing buffer (Roche, 11,814,389,001).

Depletion of mouse CD45$^+$ and CD31$^+$ cells. For mouse CD45$^+$ and CD31$^+$ cell depletion, the cells were treated with anti-mouse CD45 MicroBeads (Miltenyi Biotec, 130-052-301) and anti-mouse CD31 MicroBeads (Miltenyi Biotec, 130-097-418) and incubated at 4 °C for 20 min. Mouse CD45$^+$ and CD31$^+$ cells were depleted using the "Deplete" program of the autoMACS Pro system (Miltenyi Biotec). The negative fraction was used for flow cytometry determinations.

Flow cytometry. The CD45$^-$and CD31-depleted single-cell suspension was stained with 1 μM SYTOX Blue Dead Cell Stain; mCherry$^+$ cells were then sorted using FACSAria III (BD Biosciences).

2.13. Immunofluorescence staining

For the imaging of microfibers and mouse lungs, samples were fixed in 4% paraformaldehyde (Nacalai Tesque, 26,126–25)/PBS overnight at 4 °C. After washing with saline twice, the samples were incubated in 30% sucrose overnight at 4 °C, embedded into the OCT compound (Sakura Finetek, 4583), frozen at −80 °C, and cut into 10 μm slices. Of note, some lung samples were frozen before fixation and fixed after defrosting and cutting. The samples were permeabilized with 0.2% Triton X-100 (Nacalai Tesque, 12,969–25)/PBS for 15 min and blocked in 1% BSA (Nacalai Tesque, 01859–47)/PBS containing 5% normal donkey serum (EMD-Millipore, 566,460) for 30 min at room temperature. Slides were then incubated with primary antibodies overnight at 4 °C and stained with the respective secondary antibodies for 30 min at room temperature. Hoechst 33,342 (DOJINDO, H342) was added to the secondary antibody solution for nuclear staining. The primary and secondary antibodies used in this paper are listed in Table S1. Immunofluorescence images were obtained using the BZ-X710 system (KEYENCE) or a TCS SP8 confocal microscope (Leica Microsystems). The number of immunostained cells was quantified from 10 randomly selected fields of view per independent experiment using the Hybrid Cell Count software (BZ-H3C, KEYENCE) in the BZ-X710 system (KEYENCE). Three biological replicates from three independent experiments were used.

2.14. Imaging of whole microfibers and of the murine lungs

An entire sample was scanned automatically using the BZ-X710 system (KEYENCE); the whole sample was reconstructed from the scanned images using the BZ-X Analyzer software (KEYENCE).

2.15. Tissue clearing and 3D imaging of the lungs

Murine lung tissues were cleared as previously described [29]. In brief, samples were fixed in 4% paraformaldehyde/PBS overnight at 4 °C and washed in PBS for more than 3 h at room temperature. The samples were delipidated and permeabilized in CUBIC-L reagent [10 wt% N-butyldiethanolamine (CU#0414) (Tokyo Chemical Industry, B0725) and 10 wt% Triton X-100 (Nacalai Tesque, 12,967–45) in water] for at least three days at 37 °C with gentle shaking. The CUBIC-L reagent was changed daily or every other day during this period. The samples were

then washed in PBS for at least one day and, two days before observation were immersed in 50% CUBIC-RA reagent [45 wt% antipyrine (CU#0640) (Tokyo Chemical Industry, D1876) and 30 wt% N-methylnicotinamide (CU#1283) (Tokyo Chemical Industry, M0374) in water] for one day, followed by 100% CUBIC-RA reagent for one day at room temperature with gentle shaking. Finally, the samples were stained with 1% BSA/PBS containing 1:1000 diluted DAPI solution (DOJINDO, D523). Three-dimensional images of cleared lung tissues were obtained with the Lightsheet Z.1 fluorescence microscope (Carl Zeiss). The acquired images were reconstructed using the Imaris software (Bitplane).

2.16. Electron microscopy

Microfibers were embedded into iPGell (GenoStaff, PG20-1) according to the manufacturer's instructions. The samples were incubated in a fixing solution consisting of 2.5% glutaraldehyde (Nacalai Tesque, 17,003–92), 2% paraformaldehyde, 2% osmium tetroxide (Nacalai Tesque, 25,746–06), 0.1% picric acid (Wako, 209–08675), 4% sucrose (Nacalai Tesque, 30,404–45), and 0.1 M phosphate buffer (pH 7.4) at 4 °C for 2 h. En bloc staining was performed in 1% uranyl acetate (Merck, 8473) at room temperature for 1 h and the samples were embedded into Epon 812 to dehydrate, as previously described [10]. Ultrathin sections were stained with uranyl acetate and lead citrate and observed via H-7650 transmission electron microscopy (Hitachi).

2.17. Quantitative RT-PCR

Quantitative RT-PCR was performed on three biological replicates from three independent experiments. Total RNAs were extracted using the PureLink RNA mini kit (Thermo Fisher Scientific, 12183018A) or the NucleoSpin RNA Plus XS kit (Takara Bio, 740,990), and cDNA was synthesized from 80 ng of total RNA using SuperScript III Reverse Transcriptase (Thermo Fisher Scientific, 18,080,085) according to the manufacturer's protocol. cDNA was amplified in duplicates using the Power SYBR Green PCR Mix (Thermo Fisher Scientific, 4,368,708); the QuantStudio 3 system (Applied Biosystems) was used to quantify gene expression. The expression level of genes was normalized to that of *β-actin*. The gene expression level of each sample was compared to that of the human fetal lung at 17, 18, and 22 weeks of gestation (Agilent Technologies, #540177, Lot.0006,055,802). The primers used in this paper are described in Table S2.

2.18. RNA-seq

First-strand cDNA was synthesized and amplified from extracted total RNAs using the SMART-Seq v4 Ultra Low Input RNA kit (Takara Bio, 634,890) in accordance with the manufacturer's instructions. Sequencing libraries were prepared with the Nextera XT DNA Library Prep Kit (Illumina) and sequencing was performed using the NovaSeq 6000 sequencer (Illumina) with 100 bp paired-end reads. Raw sequencing reads were trimmed with fastp 0.20.1, and the trimmed data were mapped to the human reference genome (GRCh37/hg19) using STAR 2.7.6a. In the analysis of transplanted human cells, only reads mapped to the human reference genome were used. After mapping, RSEM 1.3.1 was used for transcript assembly, and gene expression was calculated based on read counts. RNA-seq data were analyzed using iDEP.91 [30].

2.19. Statistical analyses

Statistical analyses were performed using the GraphPad Prism 7 software (GraphPad). All error bars indicate the standard error of the mean (s.e.m.); quantitative data were obtained from three or more independent experiments. The statistical tests used are disclosed in each figure legend.

3. Results

3.1. hLPs cell-laden core-shell microfiber expansion system

Taking advantage of their self-renewal capacity, we sought to establish a method for the robust expansion of hLPs, ensuring the maintenance of their potential to differentiate into both airway and alveolar lineage cells. To facilitate cell visualization, we established an *SFTPC-GFP* knock-in reporter hiPSC line [10] stably expressing mCherry (mB2-3 cell line) (Fig. S1a, b); of note, these cells were confirmed to have a normal karyotype and to differentiate into AT2 cells using a conventional method [12] (Fig. S1c-f). Then, hLPs were stepwise induced from hPSCs on day 21, as previously reported (day 21 hLPs) [12,28] (Fig. 1a). It has been reported that three-dimensional cultures have higher scalability than two-dimensional ones [18,19]; therefore, here, we used cell-laden core-shell microfibers [23,24], as a 3D culture system to expand hLPs (Fig. 1b). Encapsulated hLPs formed aggregates in the hydrogel microfibers, proliferated whilst extending in the longitudinal direction, and finally formed a string-like structure of uniform diameter (Fig. 1c). In contrast, the cell proliferation of hLPs was poor in the context of two-dimensional cultures (Fig. S2). Importantly, four weeks after culture, quantitative RT-PCR (qRT-PCR) analysis of the hLPs expanded in the microfibers (microfiber-hLPs) revealed that the expression of the lung progenitor cell marker *NKX2.1* was maintained along with a significant increase in the expression of *SOX9* expression; for the sake of comparison, the expression of *NKX2.1* was decreased after four weeks of two-dimensional culture (Fig. 1d). Of note, a large number of microfiber-hLPs expressed both SOX9 and NKX2.1 as per immunofluorescence staining and the ratio of $SOX9^{+}$ $NKX2.1^{+}$ double-positive cells was 86.5 ± 4.3%, consistent with the previously described characteristics of human fetal lung progenitors [15,21] (Fig. 1e and f).

3.2. Evaluation of the differentiation of microfiber-hLPs in vitro

To confirm the lung progenitor potency of microfiber-hLPs, next, we evaluated the differentiation of microfiber-hLPs into both alveolar and airway epithelial cells. SFTPC-GFP-positive cells were induced with high efficiency after alveolar differentiation (Fig. S1e and Fig. 2a, b, c); the elevated expression of AT2 cell markers after alveolar differentiation was confirmed by qRT-PCR and immunofluorescence staining (Fig. 2d and e). Of note, the AT2 cell marker expression levels in alveolar-differentiated microfiber-hLPs were much higher, and the fraction of SFTPC-GFP-positive cells in flow cytometry analysis was two times greater than that in fibroblast-free alveolar organoids generated using a previously described conventional method [12] (Fig. 2c and d). Additionally, the presence of many lamellar bodies (AT2 cell-specific intracellular organelles) was confirmed via electron microscopy (Fig. 2f). The differentiation of microfiber-hLPs into airway epithelial cells was also confirmed. An increased expression of multiciliated epithelial cell markers (*FOXJ1* and *SNTN*) was detected using qRT-PCR and immunofluorescence staining (Fig. 2g and h), and multiciliated epithelial cells were observed via brightfield microscopy (Movie S1) as well as electron microscopy (Fig. 2i).

Supplementary video related to this article can be found at https://doi.org/10.1016/j.biomaterials.2021.121031

3.3. RNA-seq analysis of microfiber-hLPs and their differentiated counterparts

To examine the gene expression profile of microfiber-hLPs, we further obtained RNA-seq data (day21 hLPs, four-week microfiber-hLPs, alveolar-differentiated microfiber-hLPs, and airway-differentiated microfiber-hLPs). Principal component analysis (PCA) of these RNA-seq data suggested that microfiber-hLPs were closer to alveolar-differentiated microfiber-hLPs than to day21 hLPs (Fig. 3a).

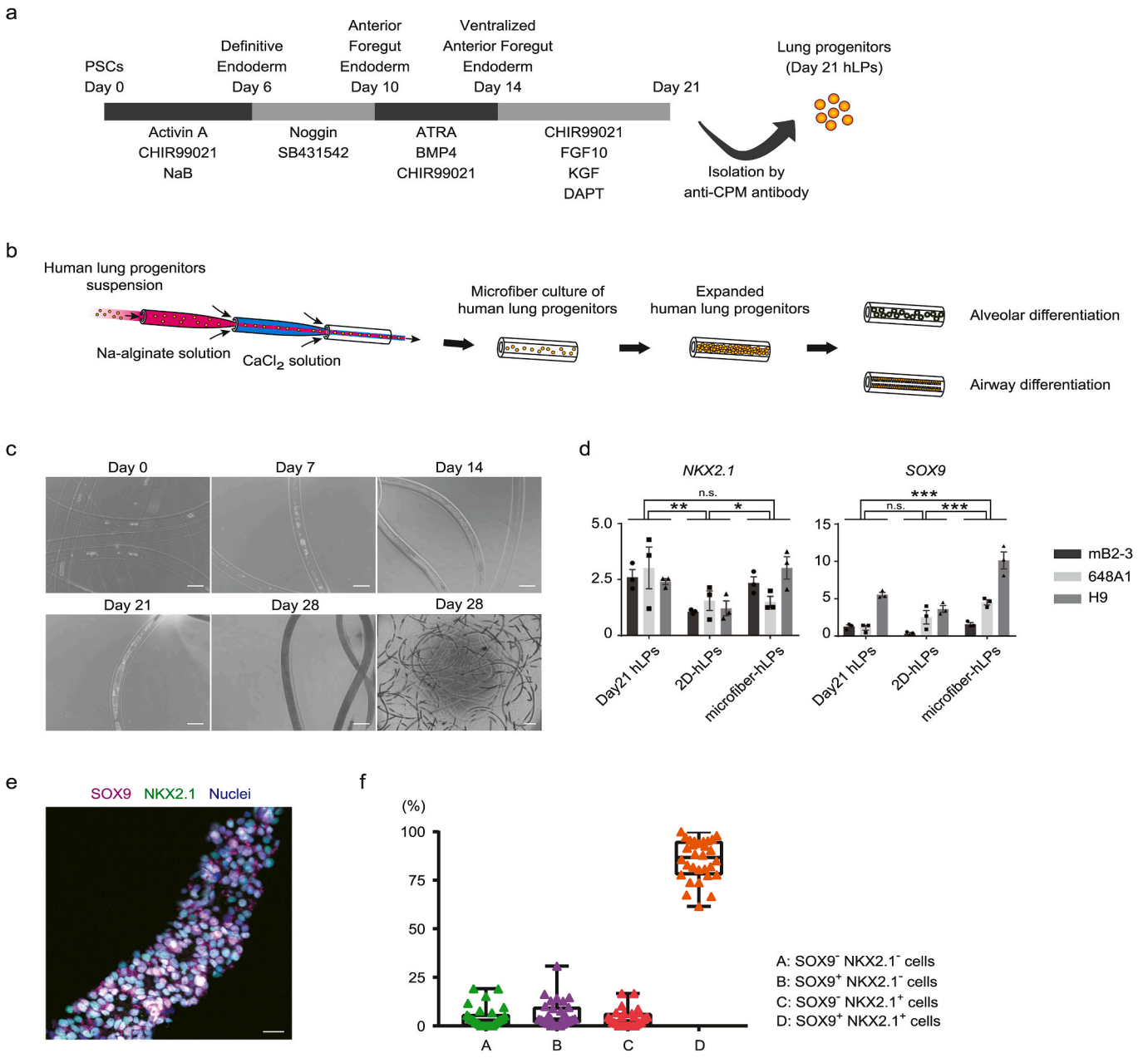

Fig. 1. Cell-laden core-shell microfiber expansion system with hLPs. (a) Schematic diagram for the stepwise induction of hPSC-derived lung progenitors on day 21 (day 21 hLPs). CPM: carboxypeptidase M. (b) Schematic illustration of the fabrication of cell-encapsulated alginate microfibers and the expansion and differentiation of hLPs into respiratory epithelial cells. (c) Time-elapsed images of the hLP proliferation in microfibers. The bottom right figure is an image of a whole microfiber on day 28. Scale bars, 500 μm (day 0, 7, 14, 21, and 28) and 5 mm (day 28, bottom right). (d) Quantitative RT-PCR (qRT-PCR) analysis of day 21 hLPs, 2D-hLPs, and microfiber-hLPs using multiple cell lines. 2D-hLPs: hLPs in two-dimensional culture for four weeks. Microfiber-hLPs: hLPs in microfibers for four weeks. Data are presented as the mean ± s. e.m. (three biological replicates from three independent experiments); statistical comparisons were performed using the two-way ANOVA with Tukey's post-hoc analysis: n. s., not significant, $*P < 0.05$, $**P < 0.01$, and $***P < 0.001$. (e) Immunofluorescence staining of hLPs expanded in microfibers. Most of the hLPs were $SOX9^+$ $NKX2.1^+$ cells. Scale bar, 25 μm. (f) The proportion of $SOX9^-$ $NKX2.1^-$ cells, $SOX9^+$ $NKX2.1^-$ cells, $SOX9^-$ $NKX2.1^+$ cells, and $SOX9^+$ $NKX2.1^+$ cells in microfiber-hLPs samples. Data are presented as the mean ± s. e.m. (n = 30 from three independent experiments). The mB2-3 hiPSC line was used in (c). The H9 hESC line was used in (e). The B2-3 hiPSC line was used in (f).

Expectedly, the heatmap showed that progenitor cell markers decreased and AT2 cell markers increased as alveolar differentiation progressed (Fig. 3b). Similarly, as airway differentiation progressed, progenitor cell markers decreased, and multiciliated epithelial markers increased (Fig. 3c). K-means clustering of the top 2000 most variable genes and enrichment analysis for each cluster also confirmed alveolar or airway cell differentiation within the microfibers (Fig. 3d and Table S3, S4).

3.4. Transplantation of day 21 hLPs into the murine lungs

To efficiently deliver drugs or cells into the murine lungs, we built an endoscope-assisted transtracheal administration system (EATAS). As a proof of principle, we used this system for the generation of drug-induced lung injured NOG mice after the administration of either bleomycin or elastase (Fig. 4a and b, and Fig. S3a, b). Importantly, the EATAS enabled the selective administration of cells into the left or right bronchi, and thus, is expected to improve the delivery efficiency of cells

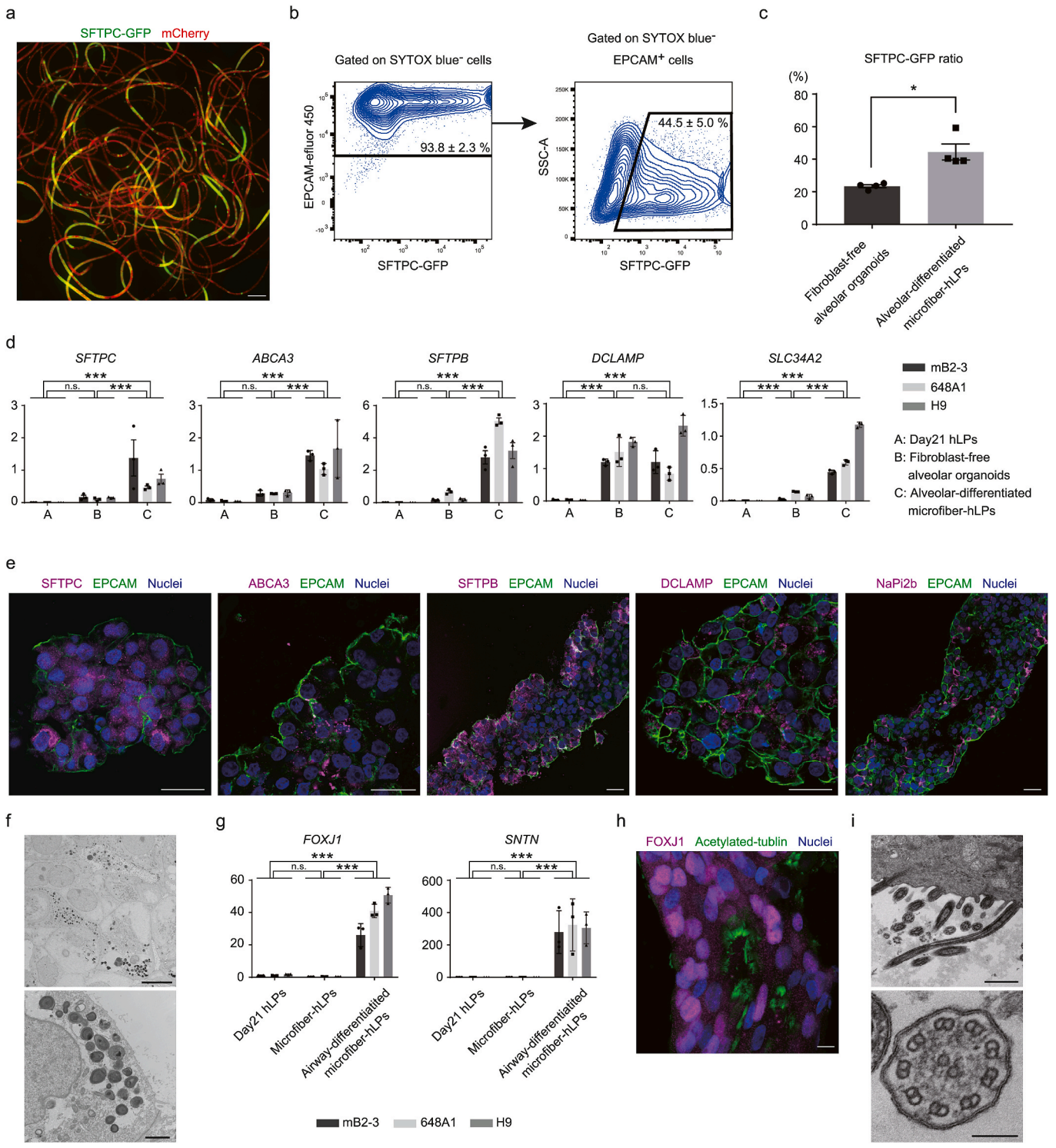

Fig. 2. Evaluation of the differentiation potency of microfiber-hLPs into the alveolar and airway epithelial lineages. (a) Live imaging of alveolar differentiation in microfibers. Scale bar, 1 mm. (b) Gating strategy for the evaluation of the alveolar differentiation of hLPs in microfibers via flow cytometry. (c) The alveolar differentiation of hLPs in microfibers resulted in a high SFTPC-GFP fraction compared with that in the context of FF-AOs. Data are presented as the mean ± s. e.m. (four biological replicates from four independent experiments). The Mann-Whitney test was used for statistical comparisons: $^{*}P < 0.05$. (d) qRT-PCR analysis of day 21 hLPs, microfiber-hLPs, and their alveolar differentiation in microfibers using multiple cell lines. Data are presented as the mean ± s. e.m. (three biological replicates from three independent experiments); statistical comparisons were performed using the two-way ANOVA with Tukey's post-hoc analysis: n. s., not significant, $^{**}P < 0.01$, and $^{***}P < 0.001$. (e) Immunofluorescence staining of alveolar-differentiated microfiber-hLPs. Various AT2 cell marker positive cells were detected in the microfibers. Scale bars, 25 μm. (f) Transmission electron microscopy (TEM) images of alveolar-differentiated microfiber-hLPs in microfibers. Scale bars, 10 μm and 2 μm. (g) qRT-PCR analysis of multiciliated epithelial cell markers in multiple cell lines. Data are presented as the mean ± s. e.m. (three biological replicates from three independent experiments); statistical comparisons were performed using the two-way ANOVA with Tukey's post-hoc analysis: n. s., not significant and $^{***}P < 0.001$. (h) Immunofluorescence image of the airway epithelial cell differentiation of hLPs. FOXJ1^{+} Acetylated tubulin^{+} cells were observed in the microfibers. Scale bar, 10 μm. (i) TEM images of the airway epithelial cell differentiation of hLPs (left: low power field, right: high power field). Scale bars, 1 μm and 100 nm. The mB2-3 hiPSC line was used in (a), (b), (c), (g), and (i). The H9 hESC line was used in (e) and (h).

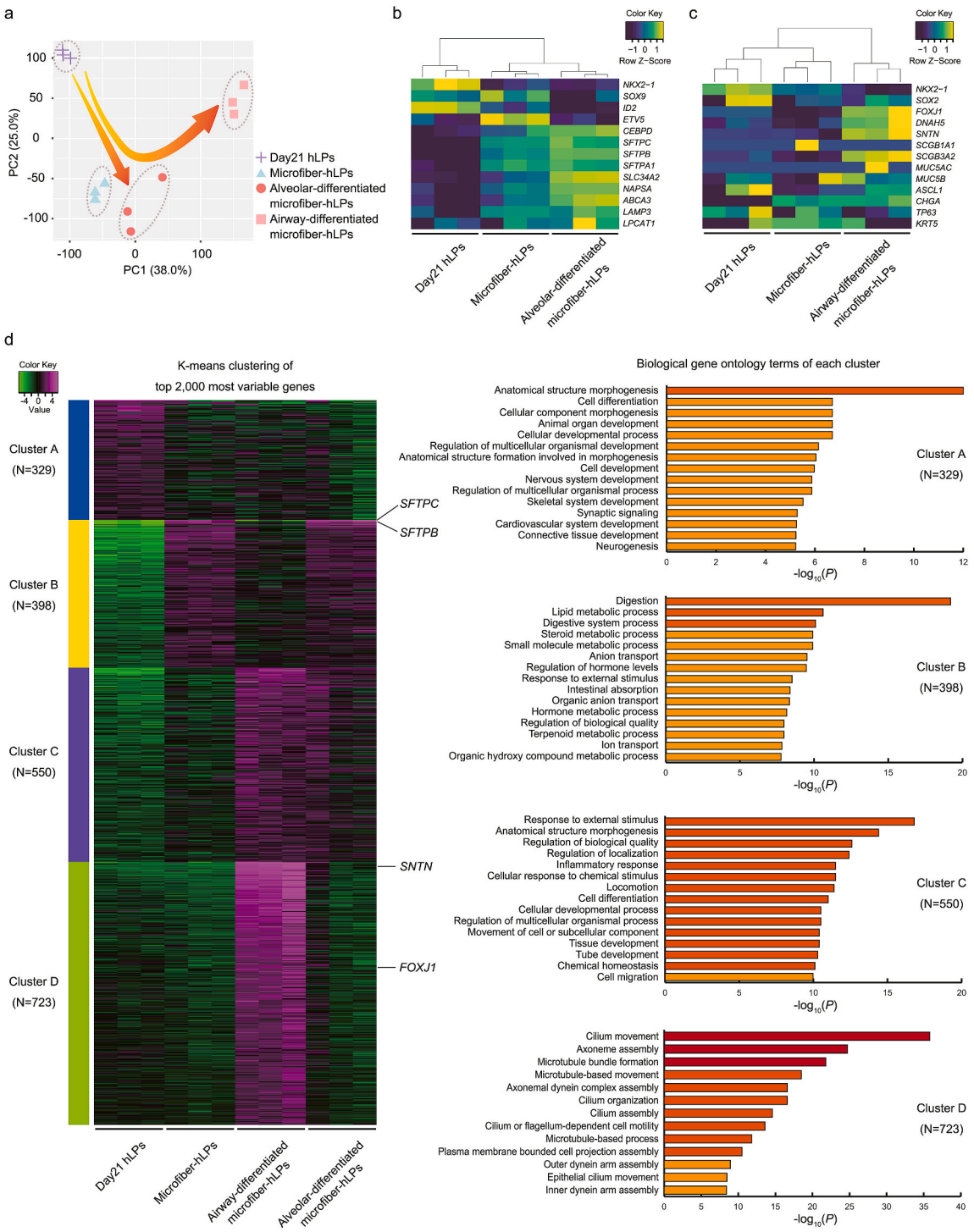

Fig. 3. RNA-seq analysis of day 21 hLPs, microfiber-hLPs, and their differentiated counterparts. (a) PCA of the RNA-seq data of day 21 hLPs, microfiber-hLPs, alveolar-differentiated microfiber-hLPs, and airway-differentiated microfiber-hLPs (three biological replicates from three independent experiments). (b) Heatmap of genes related to distal lung progenitor cells and AT2 cells on day 21 hLPs, microfiber-hLPs, and alveolar-differentiated microfiber-hLPs. (c) Heatmap of genes related to distal lung progenitor and airway epithelial cell markers on day 21 hLPs, microfiber-hLPs, and airway-differentiated microfiber-hLPs. (d) K-means clustering of the top 2000 most variable genes and biological gene ontology terms for each cluster. The mB2-3 hiPSC line was used in all experiments.

into the alveoli (Fig. 4c and Movie S2). Additionally, using the EATAS, isolated and aggregated hLPs were orthotopically transplanted into the left lung of NOG mice, treated with naphthalene two days prior to cell infusion, followed by 2.5 Gy total body irradiation 4–6 h before cell infusion (Fig. 4d). Surprisingly, the engraftment of hLPs was observed in the left lung eight weeks after transplantation (Fig. 4e). After clearing the resected lung through the CUBIC method [29], 3D imaging revealed that human cells were engrafted in clusters along the bronchi (Fig 4f, Fig. S4a, b, and Movie S3). Hematoxylin and eosin staining further revealed that the structure of the bronchi and alveoli seemed normal, and no malignant findings were observed (Fig. 4g). Interestingly, immunofluorescence staining indicated human cytokeratin-positive cell clusters in the alveolar region surrounding the bronchi, suggesting that engrafted hLPs replaced the murine lung tissues (Fig. 4g). Although

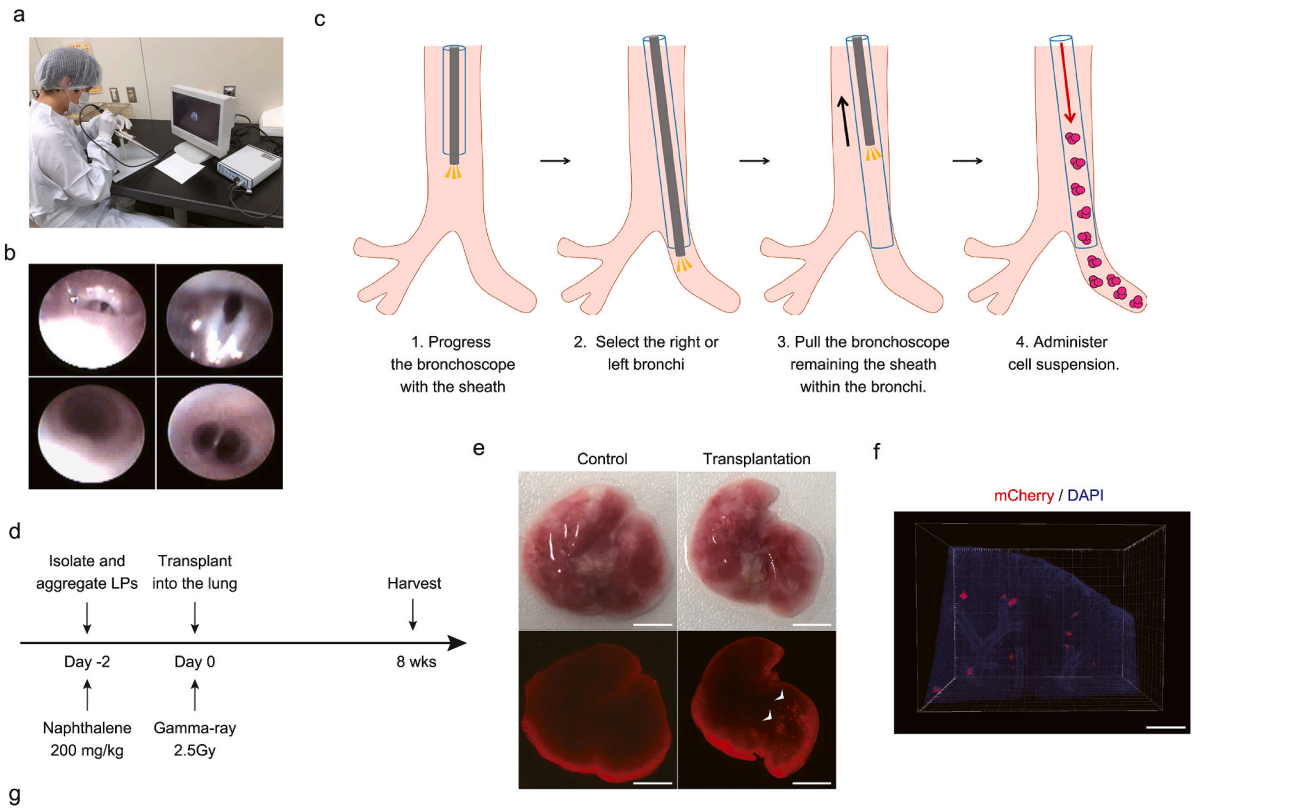

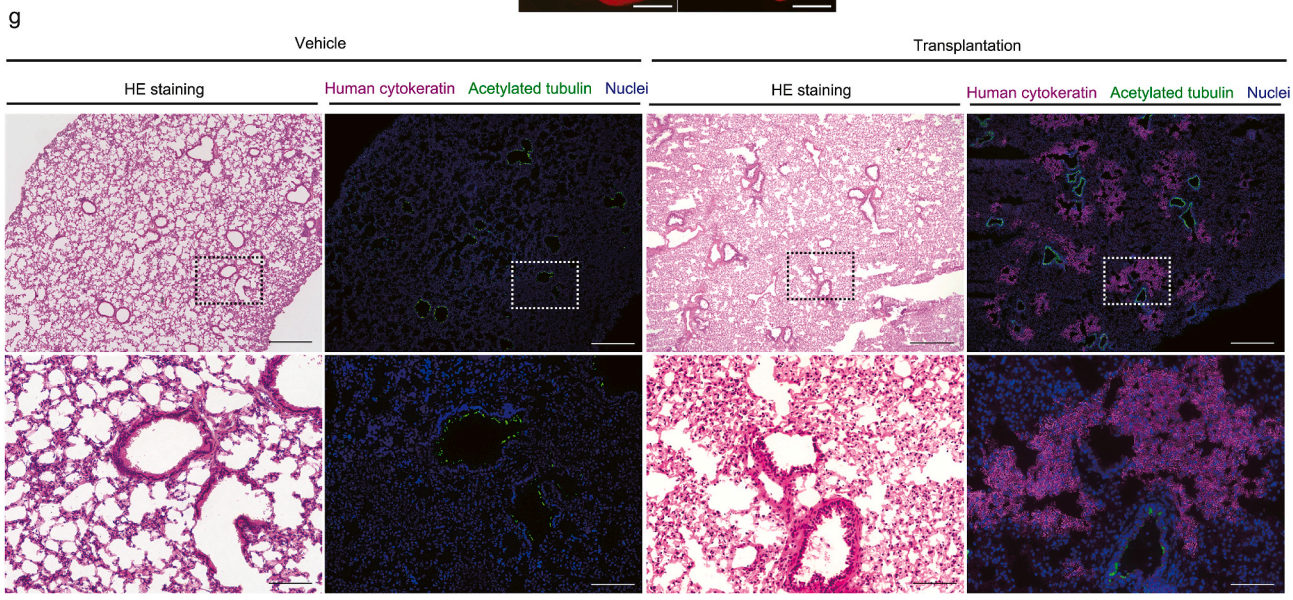

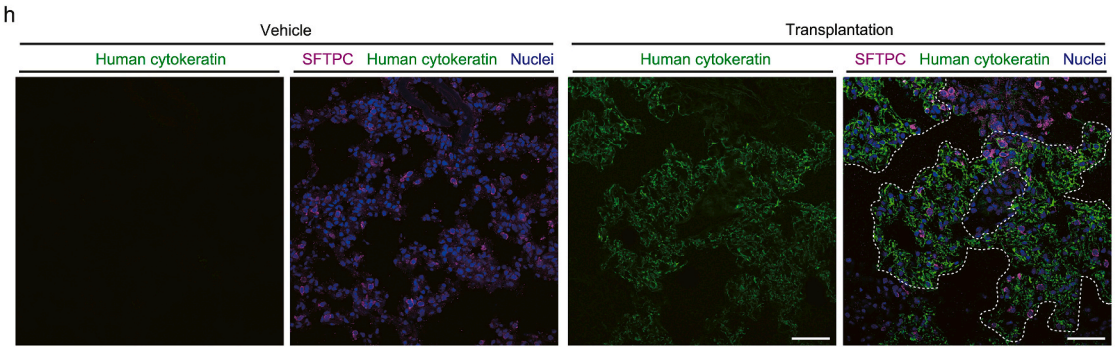

(caption on next page)

Fig. 4. Transplantation of day 21 hLPs into the murine lungs. (a) Setup for the use of the Endoscope-assisted transtracheal administration system (EATAS). (b) Bronchoscopic findings in mice. Upper images, a vocal cord; left lower image, trachea; right lower image, bifurcation of the trachea. (c) Illustration of the method of cell injection into the left lung. See Movie S2. (d) Experimental design of xenotransplantation of day 21 hLPs. (e) Live imaging of the murine lungs eight weeks after transplantation. Red cell clusters (white arrowhead) showed mCherry$^+$ human cells derived from the mB2-3 hiPSC line. Scale bar, 5 mm. (f) 3D image of cleared murine lungs with hLPs derived from mB2-3 cells. See Movie 3. (g) Hematoxylin and eosin and immunofluorescence staining of xenografts. Lower images represent the enlargement of the upper panels. Scale bars, 100 μm and 500 μm. (h) Immunofluorescence staining of engrafted hPSC-derived cells. SFTPC$^+$ cells were detected in hPSC-derived cell clusters. Scale bars, 50 μm. The mB2-3 hiPSC line was used in (e) and (f), and the B2-3 hiPSC line was used in (g) and (h).

mouse SFTPC$^+$ cells were observed outside the human cell clusters, the expression of SFTPC was also detected on engrafted cells (Fig. 4h), suggesting that injected hLPs differentiated into AT2 cells *in vivo*. As a control, we also transplanted hLPs into the murine kidney and evaluated it after eight weeks (Fig. S5a, b). Engrafted hLPs differentiated into airway epithelial cells, but not into alveolar epithelial cells (Fig. S5c, d). These results suggested that the organ-specific microenvironment is required for the differentiation of hLPs into alveolar epithelial cells.

Supplementary video related to this article can be found at https://doi.org/10.1016/j.biomaterials.2021.121031

3.5. Lineage profile of hLPs engrafted into the murine lungs

To evaluate the lineage profile of engrafted hLPs, cells were isolated from the murine lungs using mCherry-based FACS and their transcriptome was analyzed via RNA-seq (Fig. 5a and b). PCA of the RNA-seq data of day 21 hLPs, airway-differentiated microfiber-hLPs, alveolar-differentiated microfiber-hLPs, and transplanted cells revealed changes in the cell characteristics and suggested the differentiation of hLPs into respiratory epithelial cells following engraftment (Fig. 5c). Isolated engrafted cells expressed alveolar epithelial cell markers, such as AT2 cell markers (*SFTPC*, *SFTPB*, *CEACAM6*, and *SLC34A2*) and alveolar type I (AT1) cell markers (*HOPX* and *AGER*) as well as airway epithelial cell markers (*SCGB1A1*, *SCGB3A2*, and *FOXJ1*), indicative of the differentiation of hLPs into alveolar and airway epithelial cells *in vivo* (Fig. 5d and e, and Table S5). Moreover, K-means clustering of the top 1000 most variable genes and enrichment analysis in the context of each cluster revealed that the downregulated genes in engrafted cells were significantly enriched for pathways related to morphogenesis and development, while the upregulated genes were significantly enriched for pathways related to cell differentiation (Fig. S6, and Table S6, S7). Interestingly, pathways related to the response to external stimuli/immune response were significantly enriched in engrafted cells (Fig. S6). Although these findings could be due to epithelial cell injury caused by naphthalene, they may as well reflect the signals caused by xenotransplantation.

3.6. Transplantation of microfiber-hLPs into the murine lungs

Finally, we transplanted microfiber-hLPs into the lungs of mice (Fig. 6a). Stepwise differentiated hLPs were expanded via cell-laden core-shell microfiber for four weeks and were administered using the EATAS. After eight weeks, we confirmed the engraftment of microfiber-hLPs, as well as the engraftment of day 21 hLPs (Fig. 6b). We further tried to confirm the multi-lineage differentiation of engrafted cells *in vivo*, as suggested by the RNA-seq data of engrafted day 21 hLPs (Fig. 5d and e). Importantly, immunofluorescence staining indicated the differentiation of microfiber-hLPs into epithelial cells expressing AT2 (NaPi2b and SFTPC), AT1 (PDPN), and airway epithelial cell (SCGB1A1) markers, indicative of the multi-lineage differentiation of the engrafted cells *in vivo* (Fig. 6c). Overall, our results suggest we were able to differentiate the microfiber-expanded hLPs into airway and alveolar epithelial cells *in vivo* and *in vitro* (Fig. 6d).

4. Discussion

In this study, we established a cell-laden core-shell microfiber expansion culture system of hLPs allowing the maintenance of their lung progenitor traits and differentiation potency into the alveolar and airway epithelial cell lineages. Further, we demonstrated the utility of hLPs for transplantation into the murine lungs *in vivo*, and finally, achieved the transplantation of hLPs expanded via microfiber technology.

While the maintenance of lung progenitor traits was difficult, and cell proliferation was poor in two-dimensional cultures, the efficient proliferation of hLPs highly expressing the lung progenitor marker *SOX9* was observed during the four-week culture period under the fiber-based three-dimensional culture setting. Therefore, the microfiber technology not only contributed to the expansion of progenitors but also improved their quality. This is most likely because the three-dimensional environment is closer to the living body, allowing epithelial cells to grow autonomously. Of note, in previous reports of lung progenitors subjected to three-dimensional culture [21], no clear comparison was made with two-dimensional culture. Therefore, this is the first report to demonstrate that three-dimensional culture is superior to two-dimensional culture settings with regard to cell proliferation and the quality of lung progenitors. Importantly, hLPs could proliferate and differentiate appropriately in microfibers even in the absence of animal-derived scaffolds (e.g., Matrigel), thus far indispensable for conventional three-dimensional culture systems [15,21]. Because the use of Matrigel was pointed out as a limitation with respect to regenerative medicine and drug discovery purposes [31], our method is advantageous. Of note, we also discovered that microfiber-hLPs differentiated into respiratory epithelial cells, including AT2 cells, which are essential for lung regeneration, confirming that the microfiber technology allows the maintenance of the bipotency of hLPs (potential to differentiate to the alveolar and airway epithelial cell lineages). Interestingly, the microfibers enabled a more efficient differentiation into AT2 cells than that previously described in the context of a fibroblast-free method [12].

Previous reports of human cell transplantation into the murine lungs were not as consistent as papers describing the transplantation of mouse cells into mice. Miller et al. reported the engraftment of hPSC-derived cells, but the engraftment area was limited to the upper airway, and the *in vivo* differentiation of hPSC-derived cells was only evaluated via immunofluorescence staining [15]. Herein, we confirmed the patchy replacement of mouse lung cells with engrafted human cells in the alveoli. Furthermore, this is also the first report of the differentiation of hPSC-derived cells into AT2 cells *in vivo*. Additionally, also filling a gap in knowledge, we successfully isolated engrafted cells and subjected them to comprehensive transcriptomic analysis, confirming the differentiation of injected hLPs into AT2 cells as well as into other airway lineages. This represents one of the major advantages of using bipotent hLPs, because our method may be applicable to both airway (e.g., SO2-induced) and alveolar (e.g., bleomycin-induced) injury models. Considering that AT2 cells play important roles as tissue stem cells [8], we expect that this humanized lung mouse model will be a useful tool for research on lung regeneration. Of note, and importantly, we demonstrate the efficient transplantation and *in vivo* airway and alveolar differentiation not only of day21 hLPs, but also of microfiber-hLPs.

As a limitation, in this paper, Matrigel was used for hLP transplantation, although hLPs were expanded without Matrigel. Given the future of lung regeneration medicine, it is necessary to examine whether synthetic alternatives other than Matrigel can be used. Additionally, although the microfiber system-based expanded hLPs clearly showed a robust capacity to differentiate into both airway and alveolar epithelial cells, it is still not clear whether their potential outweighs that of day21 hLPs; to determine the potential differences in epithelial cell

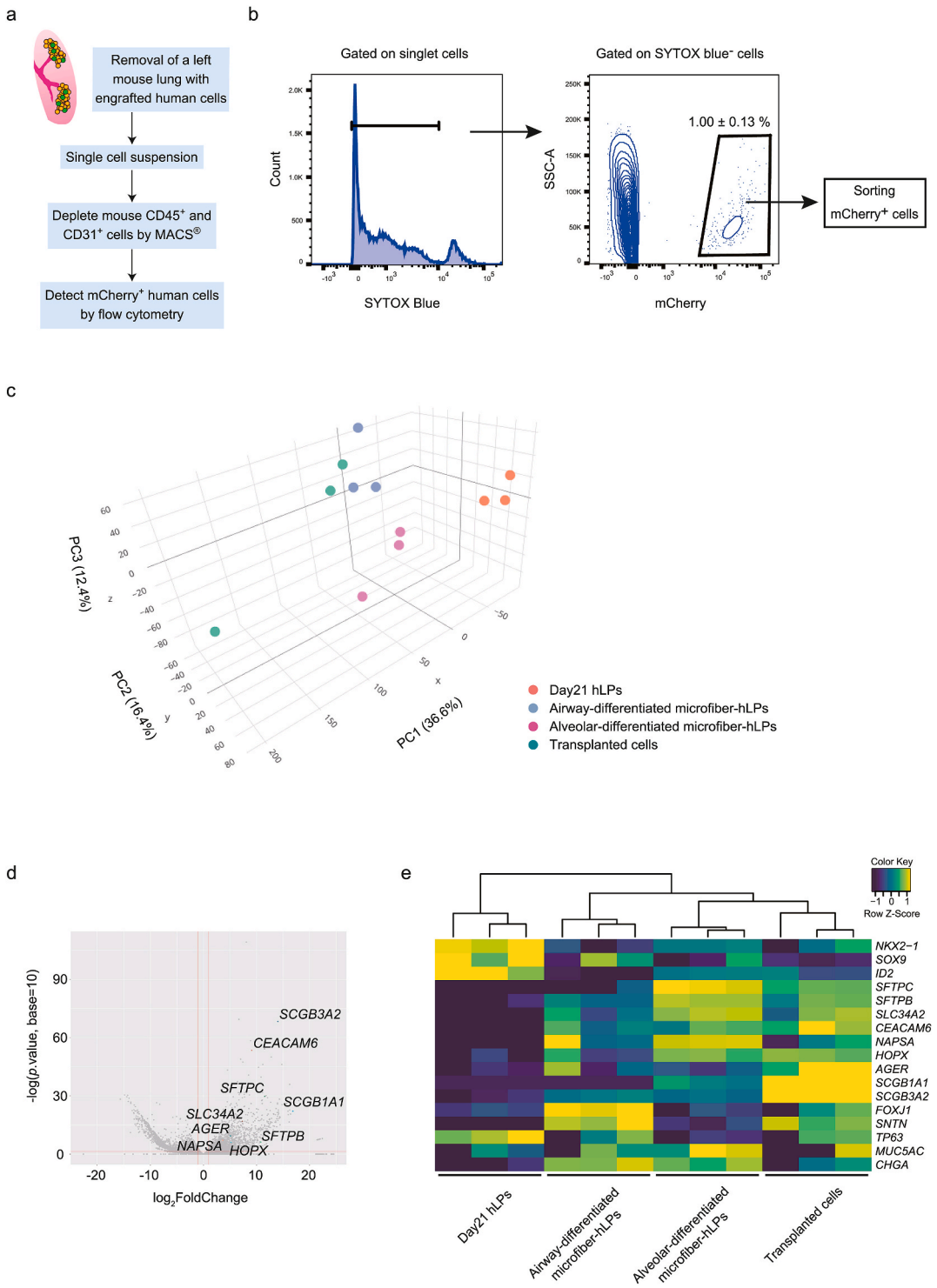

Fig. 5. Lineage profile of lung-engrafted hLPs via RNA-seq analysis. (a) Strategy used for the isolation of hPSC-derived cells from the murine lungs. (b)The gating strategy used for the fluorescence-activated cell sorting-based isolation of mB2-3-derived human cells from the murine lungs. mCherry^{+} cells were collected for transcriptomic analysis. Data are presented as the mean ± s. e.m. (three biological replicates from three independent experiments). (c) PCA of the RNA-seq data of day 21 hLPs, airway-differentiated microfiber-hLPs, alveolar-differentiated microfiber-hLPs, and transplanted cells (three biological replicates from three independent experiments). (d) Volcano plot of the differentially expressed genes between day 21 hLPs and transplanted cells. The genes representative of respiratory epithelial cells are labeled. (e) Heatmap of genes related to the distal lung progenitors and respiratory epithelial cells. The mB2-3 hiPSC line was used in all experiments.

differentiation and the engraftment efficiency is essential to clarify this issue. These studies are, therefore, the logical next step to the generation of a "more humanized" mouse model, envisioning the future human lung regeneration.

5. Conclusions

In this study, we generated a novel humanized lung mouse model using hLPs and demonstrated their differentiation into AT2 stem cells *in*

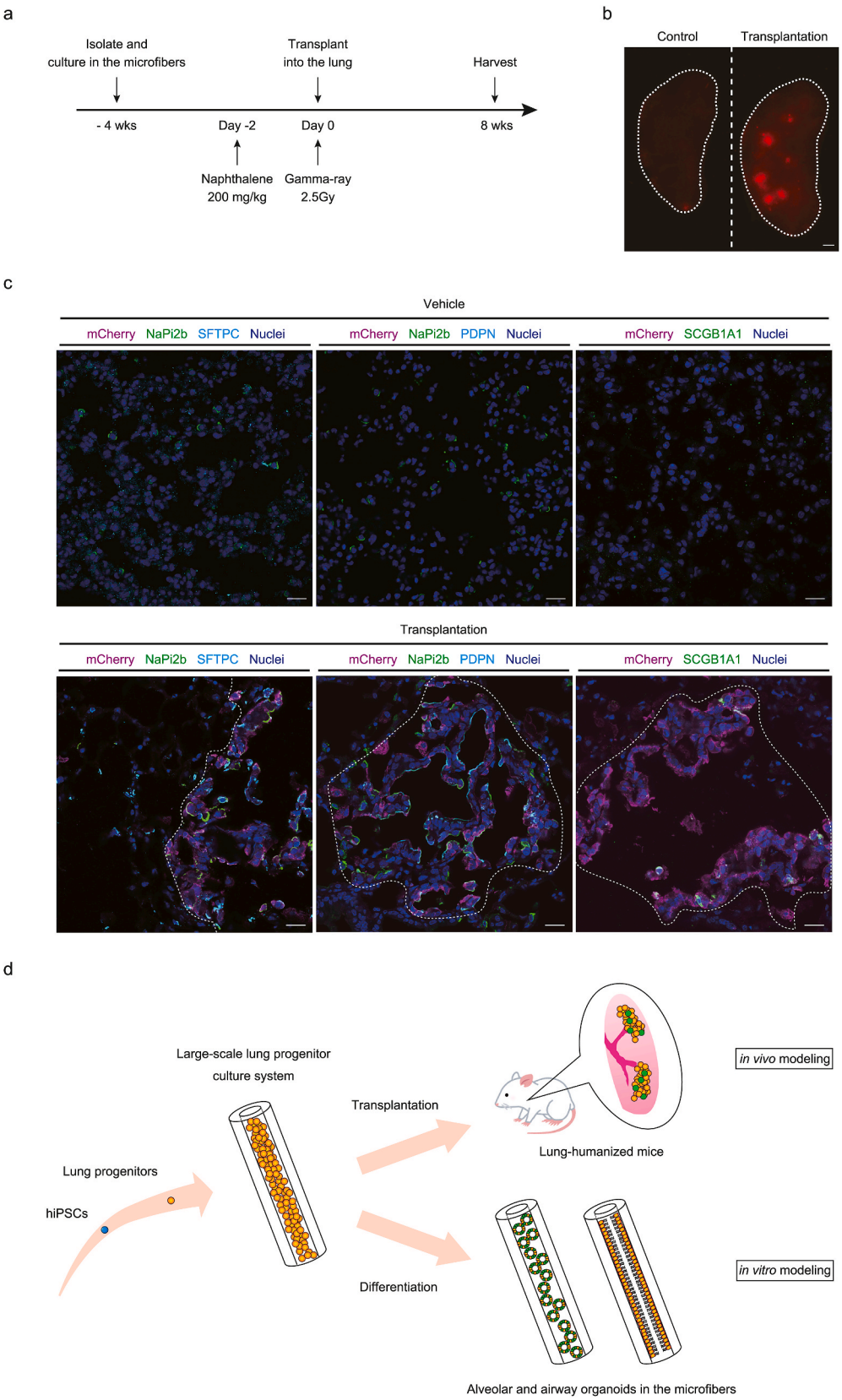

Fig. 6. Transplantation of microfiber-hLPs into the murine lungs. (a) Experimental design of the xenotransplantation of microfiber-hLPs. (b) Live imaging of the murine lungs eight weeks after the transplantation of microfiber-hLPs. Red cell clusters refer to mCherry^{+} human cells derived from the mB2-3 hiPSC line. Scale bar, 1 mm. (c) Immunofluorescence staining of grafts derived from microfiber-hLPs. HiPSCs-derived mCherry^{+} cells expressing lineage markers of AT1 (PDPN), AT2 (NaPi2b and SFTPC), and club (SCGB1A1) cells were detected in the murine lungs. Scale bars, 25 μm. (d) Strategy of the *in vivo* and *in vitro* human modeling of respiratory epithelial cells derived from hiPSCs. The mB2-3 hiPSC line was used in all experiments.

vivo. We demonstrate that hLPs can be expanded using the microfiber technology, and differentiate into AT2 cells, both *in vitro* and *in vivo*, following their transplantation into the murine lungs. Thus, the current work describes a novel regenerative medicine approach with potential for the treatment of lung diseases. In the near future, it is expected that this concept may be applied as cell therapy for respiratory diseases with no therapeutic alternative. Additionally, the high-quality hLPs and AT2 cells generated using this microfiber-based technology may be employed for drug discovery research.

Credit author statement

Satoshi Ikeo: Conceptualization, Methodology, Formal analysis, Investigation, Data curation, Writing - original draft, Visualization, Funding acquisition. **Yuki Yamamoto:** Conceptualization, Methodology, Investigation, Writing - review & editing, Visualization, Funding acquisition. **Kazuhiro Ikeda:** Methodology, Investigation, Resources, Writing - review & editing. **Naoyuki Sone:** Investigation, Writing - review & editing. **Yohei Korogi:** Investigation, Writing - review & editing. **Lucia Tomiyama:** Investigation. **Hisako Matsumoto:** Supervision, **Toyohiro Hirai:** Supervision, Funding acquisition. **Masatoshi Hagiwara:** Supervision, Funding acquisition. **Shimpei Gotoh:** Conceptualization, Writing - review & editing, Supervision, Project administration, Funding acquisition.

Declaration of competing interest

The authors declare the following financial interests/personal relationships which may be considered as potential competing interests: Kyoto University filed patents related to the methods of alveolar and airway differentiation from hPSCs. CellFiber Co., Ltd. Holds a patent on the methods of fabricating core-shell microfiber. K.I. is an employee of CellFiber Co., Ltd. Y.Y., M.H., and S.G. are founders and shareholders of HiLung Inc.

Acknowledgments

We thank S. Kanagaki, K. Moriguchi, T. Suezawa, and A. Masui (Department of Drug Discovery for Lung Diseases, Kyoto University) for technical consultation; Y. Maeda, M. Kishihata K. Tamai, N. Ikegami, and H. Yamaki for technical assistance; and K. Okamoto-Furuta and H. Kohda (Center for Anatomical Studies, Kyoto University) for electron microscopy; G. Ritter (Ludwig Institute for Cancer Research, New York City, USA) for kindly providing *anti*-NaPi2b antibody (MX35). We thank all the members of the Center for Anatomical, Pathological and Forensic Medical Research and Medical Research Support Center, Graduate School of Medicine, Kyoto University, and this work was also supported by Kyoto University Live Imaging Center. This work was supported by JSPS Fellows (19J12072 to S.I.), AMED (JP16bm0704008 and 19bm0704037 to S.G.), JSPS KAKENHI (JP17H05084 to S.G.), collaboration fund by HiLung Inc. and CellFiber Co. Ltd., in part by AMED (JP17bm0804007 to T.H.), and in part by Incubation Program from Office of Society-Academia Collaboration for Innovation, Kyoto University.

Appendix A. Supplementary data

Supplementary data to this article can be found online at https://doi.org/10.1016/j.biomaterials.2021.121031.

Data availability

All RNA-seq data in this paper were deposited in the Gene Expression Omnibus database with the accession number GSE163575.

References

[1] K.R. Parekh, J. Nawroth, A. Pai, S.M. Busch, C.N. Senger, A.L. Ryan, Stem cells and lung regeneration, Am. J. Physiol. Cell Physiol. 319 (4) (2020) C675–C693.
[2] K.A. Young, D.F. Dilling, The future of lung transplantation, Chest 155 (3) (2019) 465–473.
[3] S. Geiger, D. Hirsch, F.G. Hermann, Cell therapy for lung disease, Eur. Respir. Rev. 26 (144) (2017) 170044.
[4] A.L. Ryan, L. Ikonomou, S. Atarod, D.A. Bolukbas, J. Collins, R. Freishtat, F. Hawkins, S.E. Gilpin, F.E. Uhl, J.J. Uriarte, D.J. Weiss, D.E. Wagner, Stem cells, cell therapies, and bioengineering in lung biology and diseases 2017. An official American thoracic society workshop report, Am. J. Respir. Cell Mol. Biol. 61 (4) (2019) 429–439.
[5] M.A. Matthay, C.S. Calfee, H. Zhuo, B.T. Thompson, J.G. Wilson, J.E. Levitt, A. J. Rogers, J.E. Gotts, J.P. Wiener-Kronish, E.K. Bajwa, M.P. Donahoe, B.J. McVerry, L.A. Ortiz, M. Exline, J.W. Christman, J. Abbott, K.L. Delucchi, L. Caballero, M. McMillan, D.H. McKenna, K.D. Liu, Treatment with allogeneic mesenchymal stromal cells for moderate to severe acute respiratory distress syndrome (START study): a randomised phase 2a safety trial, Lancet Respir. Med. 7 (2) (2019) 154–162.
[6] M.K. Glassberg, J. Minkiewicz, R.L. Toonkel, E.S. Simonet, G.A. Rubio, D. DiFede, S. Shafazand, A. Khan, M.V. Pujol, V.F. LaRussa, L.H. Lancaster, G.D. Rosen, J. Fishman, Y.N. Mageto, A. Mendizabal, J.M. Hare, Allogeneic human mesenchymal stem cells in patients with idiopathic pulmonary fibrosis via intravenous delivery (AETHER): a phase I safety clinical trial, Chest 151 (5) (2017) 971–981.
[7] D.J. Weiss, R. Casaburi, R. Flannery, M. LeRoux-Williams, D.P. Tashkin, A placebo-controlled, randomized trial of mesenchymal stem cells in COPD, Chest 143 (6) (2013) 1590–1598.
[8] C.E. Barkauskas, M.J. Cronce, C.R. Rackley, E.J. Bowie, D.R. Keene, B.R. Stripp, S. H. Randell, P.W. Noble, B.L. Hogan, Type 2 alveolar cells are stem cells in adult lung, J. Clin. Invest. 123 (7) (2013) 3025–3036.
[9] Z. Borok, S.I. Danto, R.L. Lubman, Y. Cao, M.C. Williams, E.D. Crandall, Modulation of T1α expression with alveolar epithelial cell phenotype in vitro, Am. J. Physiol. Lung Cell Mol. Physiol. 275 (1) (1998) L155–L164.
[10] S. Gotoh, I. Ito, T. Nagasaki, Y. Yamamoto, S. Konishi, Y. Korogi, H. Matsumoto, S. Muro, T. Hirai, M. Funato, S. Mae, T. Toyoda, A. Sato-Otsubo, S. Ogawa, K. Osafune, M. Mishima, Generation of alveolar epithelial spheroids via isolated progenitor cells from human pluripotent stem cells, Stem Cell Rep 3 (3) (2014) 394–403.
[11] S. Konishi, S. Gotoh, K. Tateishi, Y. Yamamoto, Y. Korogi, T. Nagasaki, H. Matsumoto, S. Muro, T. Hirai, I. Ito, S. Tsukita, M. Mishima, Directed induction of functional multi-ciliated cells in proximal airway epithelial spheroids from human pluripotent stem cells, Stem Cell Rep 6 (1) (2016) 18–25.
[12] Y. Yamamoto, S. Gotoh, Y. Korogi, M. Seki, S. Konishi, S. Ikeo, N. Sone, T. Nagasaki, H. Matsumoto, S. Muro, I. Ito, T. Hirai, T. Kohno, Y. Suzuki, M. Mishima, Long-term expansion of alveolar stem cells derived from human iPS cells in organoids, Nat. Methods 14 (11) (2017) 1097–1106.
[13] S.X. Huang, M.N. Islam, J. O'Neill, Z. Hu, Y.G. Yang, Y.W. Chen, M. Mumau, M. D. Green, G. Vunjak-Novakovic, J. Bhattacharya, H.W. Snoeck, Efficient generation of lung and airway epithelial cells from human pluripotent stem cells, Nat. Biotechnol. 32 (1) (2014) 84–91.
[14] A. Jacob, M. Morley, F. Hawkins, K.B. McCauley, J.C. Jean, H. Heins, C.L. Na, T. E. Weaver, M. Vedaie, K. Hurley, A. Hinds, S.J. Russo, S. Kook, W. Zacharias, M. Ochs, K. Traber, L.J. Quinton, A. Crane, B.R. Davis, F.V. White, J. Wambach, J. A. Whitsett, F.S. Cole, E.E. Morrisey, S.H. Guttentag, M.F. Beers, D.N. Kotton, Differentiation of human pluripotent stem cells into functional lung alveolar epithelial cells, Cell Stem Cell 21 (4) (2017) 472–488 e10.
[15] A.J. Miller, D.R. Hill, M.S. Nagy, Y. Aoki, B.R. Dye, A.M. Chin, S. Huang, F. Zhu, E. S. White, V. Lama, J.R. Spence, In vitro induction and *in vivo* engraftment of lung bud tip progenitor cells derived from human pluripotent stem cells, Stem Cell Rep 10 (1) (2018) 101–119.
[16] M. Mandai, A. Watanabe, Y. Kurimoto, Y. Hirami, C. Morinaga, T. Daimon, M. Fujihara, H. Akimaru, N. Sakai, Y. Shibata, M. Terada, Y. Nomiya, S. Tanishima, M. Nakamura, H. Kamao, S. Sugita, A. Onishi, T. Ito, K. Fujita, S. Kawamata, M. J. Go, C. Shinohara, K.I. Hata, M. Sawada, M. Yamamoto, S. Ohta, Y. Ohara, K. Yoshida, J. Kuwahara, Y. Kitano, N. Amano, M. Umekage, F. Kitaoka, A. Tanaka, C. Okada, N. Takasu, S. Ogawa, S. Yamanaka, M. Takahashi, Autologous induced stem-cell-derived retinal cells for macular degeneration, N. Engl. J. Med. 376 (11) (2017) 1038–1046.
[17] T. Kikuchi, A. Morizane, D. Doi, H. Magotani, H. Onoe, T. Hayashi, H. Mizuma, S. Takara, R. Takahashi, H. Inoue, S. Morita, M. Yamamoto, K. Okita, M. Nakagawa, M. Parmar, J. Takahashi, Human iPS cell-derived dopaminergic neurons function in a primate Parkinson's disease model, Nature 548 (7669) (2017) 592–596.
[18] M. Serra, C. Brito, C. Correia, P.M. Alves, Process engineering of human pluripotent stem cells for clinical application, Trends Biotechnol. 30 (6) (2012) 350–359.
[19] Y. Lei, D.V. Schaffer, A fully defined and scalable 3D culture system for human pluripotent stem cell expansion and differentiation, Proc. Natl. Acad. Sci. U. S. A 110 (52) (2013) E5039–E5048.
[20] A.J. Miller, B.R. Dye, D. Ferrer-Torres, D.R. Hill, A.W. Overeem, L.D. Shea, J. R. Spence, Generation of lung organoids from human pluripotent stem cells in vitro, Nat. Protoc. 14 (2) (2019) 518–540.
[21] M.Z. Nikolić, O. Caritg, Q. Jeng, J.-A. Johnson, D. Sun, K.J. Howell, J.L. Brady, U. Laresgoiti, G. Allen, R. Butler, M. Zilbauer, A. Giangreco, E.L. Rawlins, Human

embryonic lung epithelial tips are multipotent progenitors that can be expanded in vitro as long-term self-renewing organoids, eLife 6 (2017), e26575.
[22] J. van der Vaart, H. Clevers, Airway organoids as models of human disease, J. Intern. Med. 289 (5) (2020) 604–613.
[23] H. Onoe, T. Okitsu, A. Itou, M. Kato-Negishi, R. Gojo, D. Kiriya, K. Sato, S. Miura, S. Iwanaga, K. Kuribayashi-Shigetomi, Y.T. Matsunaga, Y. Shimoyama, S. Takeuchi, Metre-long cell-laden microfibres exhibit tissue morphologies and functions, Nat. Mater. 12 (6) (2013) 584–590.
[24] K. Ikeda, S. Nagata, T. Okitsu, S. Takeuchi, Cell fiber-based three-dimensional culture system for highly efficient expansion of human induced pluripotent stem cells, Sci. Rep. 7 (1) (2017) 2850.
[25] K. Takahashi, K. Tanabe, M. Ohnuki, M. Narita, T. Ichisaka, K. Tomoda, S. Yamanaka, Induction of pluripotent stem cells from adult human fibroblasts by defined factors, Cell 131 (5) (2007) 861–872.
[26] K. Okita, T. Yamakawa, Y. Matsumura, Y. Sato, N. Amano, A. Watanabe, N. Goshima, S. Yamanaka, An efficient nonviral method to generate integration-free human-induced pluripotent stem cells from cord blood and peripheral blood cells, Stem Cell. 31 (3) (2013) 458–466.
[27] J.A. Thomson, J. Itskovitz-Eldor, S.S. Shapiro, M.A. Waknitz, J.J. Swiergiel, V. S. Marshall, J.M. Jones, Embryonic stem cell lines derived from human blastocysts, Science 282 (5391) (1998) 1145–1147.
[28] Y. Korogi, S. Gotoh, S. Ikeo, Y. Yamamoto, N. Sone, K. Tamai, S. Konishi, T. Nagasaki, H. Matsumoto, I. Ito, T.F. Chen-Yoshikawa, H. Date, M. Hagiwara, I. Asaka, A. Hotta, M. Mishima, T. Hirai, In vitro disease modeling of hermansky-pudlak syndrome type 2 using human induced pluripotent stem cell-derived alveolar organoids, Stem Cell Rep 12 (3) (2019) 431–440.
[29] K. Tainaka, T.C. Murakami, E.A. Susaki, C. Shimizu, R. Saito, K. Takahashi, A. Hayashi-Takagi, H. Sekiya, Y. Arima, S. Nojima, M. Ikemura, T. Ushiku, Y. Shimizu, M. Murakami, K.F. Tanaka, M. Iino, H. Kasai, T. Sasaoka, K. Kobayashi, K. Miyazono, E. Morii, T. Isa, M. Fukayama, A. Kakita, H.R. Ueda, Chemical landscape for tissue clearing based on hydrophilic reagents, Cell Rep. 24 (8) (2018) 2196–2210 e9.
[30] S.X. Ge, E.W. Son, R. Yao, iDEP: an integrated web application for differential expression and pathway analysis of RNA-Seq data, BMC Bioinf. 19 (1) (2018) 534.
[31] E.A. Aisenbrey, W.L. Murphy, Synthetic alternatives to Matrigel, Nat Rev Mater 5 (7) (2020) 539–551.